
Disentangled Generative Graph Representation Learning

Xinyue Hu

Xidian University

xinyuehu122@gmail.com

Zhibin Duan

Xidian University

xd_zhibin@163.com

Xinyang Liu

Xidian University

xinyangATK@gmail.com

Yuxin Li

Xidian University

yuxinli2020@gmail.com

Bo Chen*

Xidian University

bchen@mail.xidian.edu.com

Mingyuan Zhou

The University of Texas at Austin

mingyuan.zhou@mccombs.utexas.edu

Abstract

Recently, generative graph models have shown promising results in learning graph representations through self-supervised methods. However, most existing generative graph representation learning (GRL) approaches rely on random masking across the entire graph, which overlooks the entanglement of learned representations. This oversight results in non-robustness and a lack of explainability. Furthermore, disentangling the learned representations remains a significant challenge and has not been sufficiently explored in GRL research. Based on these insights, this paper introduces **DiGGR** (**D**isentangled **G**enerative **G**raph **R**epresentation **L**earning), a self-supervised learning framework. DiGGR aims to learn latent disentangled factors and utilizes them to guide graph mask modeling, thereby enhancing the disentanglement of learned representations and enabling end-to-end joint learning. Extensive experiments on 11 public datasets for two different graph learning tasks demonstrate that DiGGR consistently outperforms many previous self-supervised methods, verifying the effectiveness of the proposed approach.

1 Introduction

Self-supervised learning (SSL) has received much attention due to its appealing capacity for learning data representation without label supervision. While contrastive SSL approaches are becoming increasingly utilized on images [Chen et al., 2020] and graphs [You et al., 2020], generative SSL has been gaining significance, driven by groundbreaking practices such as BERT for language [Devlin et al., 2018], BEiT [Bao et al., 2021], and MAE [He et al., 2022a] for images. Along this line, there is a growing interest in constructing generative SSL models for other modalities, such as graph masked autoencoders (GMAE). Generally, the fundamental concept of GMAE [Tan et al., 2022] is to utilize an autoencoder architecture to reconstruct input node features, structures, or both, which are randomly masked before the encoding step. Recently, various well-designed GMAEs have emerged, achieving remarkable results in both node classification and graph classification [Hou et al., 2022, Tu et al., 2023, Tian et al., 2023].

*Corresponding author

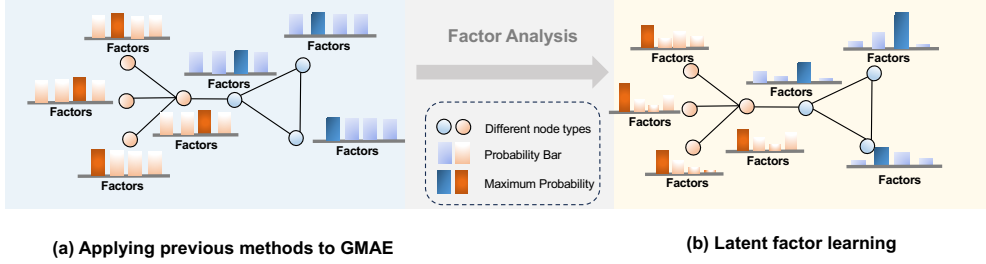


Figure 1: The number of latent factors is set to 4. In Fig. 1(a), the probabilities of nodes belonging to different latent groups are similar, resulting in nodes of the same type being incorrectly assigned to different factors. In contrast, Fig. 1(b) shows that the probabilities of node-factor affiliation are more discriminative, correctly categorizing nodes of the same type into the same latent group.

Despite their significant achievements, most GMAE approaches typically treat the entire graph as holistic, ignoring the graph’s latent structure. As a result, the representation learned for a node tends to encapsulate the node’s neighborhood as a perceptual whole, disregarding the nuanced distinctions between different parts of the neighborhood [Ma et al., 2019, Li et al., 2021, Mo et al., 2023]. For example, in a social network G , individual n is a member of both a mathematics group and several sports interest groups. Due to the diversity of these different communities, she may exhibit different characteristics when interacting with members from various communities. Specifically, the information about the mathematics group may be related to her professional research, while the information about sports clubs may be associated with her hobbies. However, the existing approach overlooks the heterogeneous factors of node n , failing to identify and disentangle these pieces of information effectively [Hou et al., 2022]. Consequently, the learned features may be easily influenced by irrelevant factors, resulting in poor robustness and difficulty in interpretation.

To alleviate the challenge described above, there is an increasing interest in disentangled graph representation learning [Bengio et al., 2013, Li et al., 2021, Ma et al., 2019, Mo et al., 2023, Xiao et al., 2022], which aims at acquiring representations that can disentangle the underlying explanatory factors of variation in the graph. Specifically, many of these methods rely on a latent factor detection module, which learns the latent factors of each node by comparing node representations with various latent factor prototypes. By leveraging these acquired latent factors, these models adeptly capture factor-wise graph representations, effectively encapsulating the latent structure of the graph. Despite significant progress, few studies have endeavored to adapt these methods to generative graph representation learning methods, such as GMAE. This primary challenge arises from the difficulty of achieving convergence in the latent factor detection module under the generative training target, thus presenting obstacles in practical implementation. As shown in Fig. 1(a), directly applying the previous factor learning method to GMAE would make the factor learning module difficult to converge, resulting in undistinguished probabilities and misallocation of similar nodes to different latent factor groups.

To address these challenges, we introduce **Disentangled Generative Graph Representation Learning (DiGGR)**, a self-supervised graph generation representation learning framework. Generally speaking, DiGGR learns how to generate graph structures from latent disentangled factors z and leverages this to guide graph mask reconstruction, while enabling end-to-end joint learning. Specifically, *i*) To capture the heterogeneous factors in the nodes, we introduce the latent factor learning module. This module models how edges and nodes are generated from latent factors, allowing graphs to be factorized into multiple disentangled subgraphs. *ii*) To learn a deeper disentangled graph representation, we design a factor-wise self-supervised graph representation learning framework. For each subgraph, we employ a distinct masking strategy to learn an improved factor-specific graph representation. Evaluation shows that the proposed framework can achieve significant performance enhancement on various node and graph classification benchmarks.

The main contributions of this paper can be summarized as follows:

- We utilized the latent disentangled factor to guide mask modeling. A probabilistic graph generation model is employed to identify the latent factors within a graph, and it can be jointly trained with GMAE through variational inference.

- Introducing **DiGGR (Disentangled Generative Graph Representation Learning)** to further capture the disentangled information in the latent factors, enhancing the disentanglement of the learned node representations.
- Empirical results show that the proposed DiGGR outperforms many previous self-supervised methods in various node- and graph-level classification tasks.

2 Related works

Graph Self-Supervised Learning: Graph SSL has achieved remarkable success in addressing label scarcity in real-world network data, mainly consisting of contrastive and generative methods. Contrastive methods, includes feature-oriented approaches[Hu et al., 2019, Zhu et al., 2020, Veličković et al., 2018], proximity-oriented techniques [Hassani and Khasahmadi, 2020, You et al., 2020], and graph-sampling-based methods [Qiu et al., 2020]. A common limitation across these approaches is their heavy reliance on the design of pretext tasks and augmentation techniques. Compared to contrastive methods, generative methods are generally simpler to implement. Recently, to tackle the challenge of overemphasizing neighborhood information at the expense of structural information [Hassani and Khasahmadi, 2020, Veličković et al., 2018], the Graph Masked Autoencoder (GMAE) has been proposed. It applies a masking strategy to graph structure [Li et al., 2023a], node attributes [Hou et al., 2022], or both [Tian et al., 2023] for representation learning. Unlike most GMAEs, which employ random mask strategies, this paper builds disentangled mask strategies.

Disentangled Graph Learning: Disentangled representation learning aims to discover and isolate the fundamental explanatory factors inherent in the data [Bengio et al., 2013]. Existing efforts in disentangled representation learning have primarily focused on computer vision [Higgins et al., 2017, Jiang et al., 2020]. Recently, there has been a surge of interest in applying these techniques to graph-structured data [Li et al., 2021, Ma et al., 2019, Mercatali et al., 2022, Mo et al., 2023]. For example, DisenGCN [Ma et al., 2019] utilizes an attention-based methodology to discriminate between distinct latent factors, enhancing the representation of each node to more accurately reflect its features across multiple dimensions. DGCL [Li et al., 2021] suggests learning disentangled graph-level representations through self-supervision, ensuring that the factorized representations independently capture expressive information from various latent factors. Despite the excellent results achieved by the aforementioned methods on various tasks, these methods are difficult to converge in generative graph SSL, as we demonstrated in the experiment of Table.3. Therefore, this paper proposes a disentangled-guided framework for generative graph representation learning, capable of learning disentangled representations in an end-to-end self-supervised manner.

3 Proposed Method

In this section, we propose **DiGGR (Disentangled Generative Graph Representation Learning)** for self-supervised graph representation learning with mask modeling. The framework was depicted in Figure 2, comprises three primary components: Latent Factor Learning (Section 3.2), Graph Factorization (Section 3.2) and Disentangled Graph Masked autoencoder (Section 3.3). Before elaborating on them, we first show some notations.

3.1 Preliminaries

A graph G can be represented as a multi-tuple $\mathcal{G} = \{V, A, X\}$ with N nodes and M edges, where $|V| = N$ is the node set, $|A| = M$ is the edge set, and $X \in \mathbb{R}^{N \times L}$ is the feature matrix for N nodes with L dimensional feature vector. The topology structure of graph G can be found in its adjacency matrix $A \in \mathbb{R}^{N \times N}$. $z \in \mathbb{R}^{N \times K}$ is the latent disentangled factor matrix, and K is the predefined factor number. Since we aim to obtain the z to guide the mask modeling, we first utilize a probabilistic graph generation model to factorize the graph before employing the mask mechanism. Given the graph G , it is factorized into $\{G_1, G_2, \dots, G_K\}$, and each factor-specific graph G_k consists of its factor-specific edges $A^{(k)}$, node set $V^{(k)}$ and node feature matrix $X^{(k)}$. Other notations will be elucidated as they are employed.

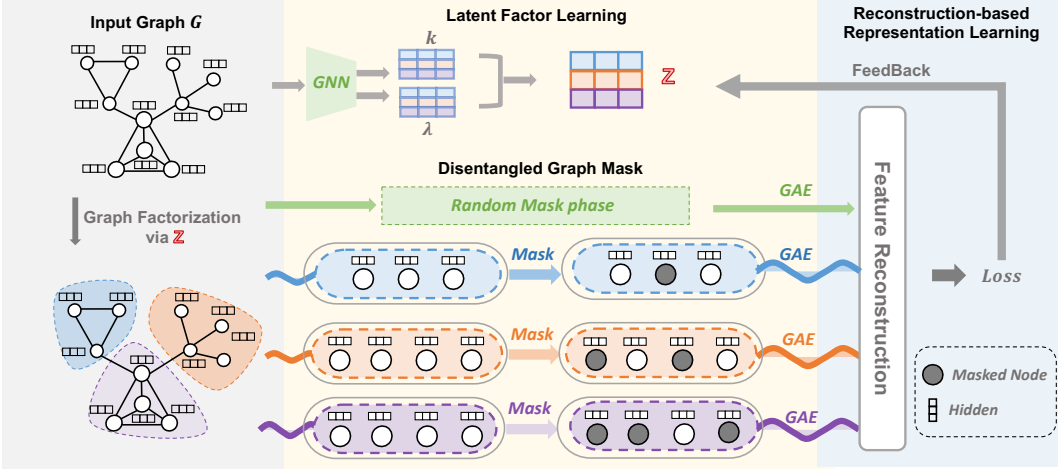


Figure 2: The overview of proposed DiGGR’s computation graph. The input data successively passes three modules described in Sections 3.2 and 3.3: Latent Factor Learning, Graph Factorization, and Disentangled Graph Mask Autoencoder. Graph information will be first processed through Latent Factor Learning and Graph Factorization, the former processed the input graph to get the latent factor z ; the latter performs graph factorization via z , such that in each factorized subgraph, nodes exchange more information with intensively interacted neighbors. Hence, during the disentangled graph masking phase, we will individually mask each factorized subgraph to enhance the disentanglement of the obtained node representations.

3.2 Latent Factor Learning

In this subsection, we describe the latent factor learning method. In this phase, our objective is to derive factor-specific node sets $\{V^{(1)}, V^{(2)}, \dots, V^{(K)}\}$ and adjacency matrices $\{A^{(1)}, A^{(2)}, \dots, A^{(K)}\}$, serving as basic unit of the graph to guide the subsequent masking. The specific approach involves modeling the distribution of nodes and edges, utilizing the generative process developed in EPM [Zhou, 2015]. The generative process of EPM under the Bernoulli-Poisson link [Zhou, 2015, Duan et al., 2021] can be described as:

$$M_{uv} \sim \text{Poisson}(\sum_{k=1}^K \gamma_k z_{uk} z_{vk}), \quad z_{uk} \sim \text{Gamma}(\alpha, \beta), \quad u, v \in [1, N] \quad (1)$$

where K is the predefined number of latent factors, and u and v are the indexes of the nodes. Here, M_{uv} is the latent count variable between node u and v ; γ_k is a positive factor activation level indicator, which measures the node interaction frequency via factor k ; z_{uk} is a positive latent variable for node u , which measures how strongly node u is affiliated with factor k . The prior distribution of latent factor variable z_{uk} is set to Gamma distribution, where α and β are normally set to 1. Therefore, the intuitive explanation for this generative process is that, with z_{uk} and z_{vk} measuring how strongly node u and v are affiliated with the k -th factor, respectively, the product $\gamma_k z_{uk} z_{vk}$ measures how strongly nodes u and v are connected due to their affiliations with the k -th factor.

Node Factorization: Equation 1 can be further augmented as follows:

$$M_{uv} = \sum_k M_{ukv}, \quad M_{ukv} \sim \text{Poisson}(\gamma_k z_{uk} z_{vk}) \quad (2)$$

where M_{ukv} represents how often nodes u and v interact due to their affiliations with the k -th factor. To represent how often node u is affiliated with the k -th factor, we further introduce the latent count $M_{uk.} = \sum_{v \neq u} M_{ukv}$. Then, we can soft assign node u to multiple factors in $\{k : M_{uk.} \geq 1\}$, or hard assign node u to a single factor using $\arg \max_k (M_{uk.})$. However, our experiments show that

soft assignment method results in significant overlap among node sets from different factor group, diminishing the distinctiveness. Note that previous study addressed a similar issue by selecting the top- k most attended regions [Kakogeorgiou et al., 2022]. Thus, we choose the hard assign strategy to factorize the graph node set V graph into factor-specific node sets $\{V^{(1)}, V^{(2)}, \dots, V^{(K)}\}$.

Edge Factorization: To create factor-specific edges $A^{(k)}$ for a factor-specific node set $V^{(k)}$, a straightforward method involves removing all external nodes connected to other factor groups. This can be defined as:

$$A_{uv}^{(k)} = \begin{cases} A_{uv}, & \forall u, v \in V^{(k)}; u, v \in [1, N]; \\ 0, & \exists u, v \notin V^{(k)}; u, v \in [1, N]. \end{cases} \quad (3)$$

Besides, the global graph edge A can also be factorized into positive-weighted edges [He et al., 2022b] for each latent factor as:

$$A_{uv}^{(k)} = A_{uv} \cdot \frac{\exp(\gamma_k z_{uk} z_{vk})}{\sum_{k'} \exp(\gamma_{k'} z_{uk'} z_{vk'})}; \quad k \in [1, K], u, v \in [1, N]. \quad (4)$$

Applying Equation 4 to all pairs of nodes yields weighted adjacency matrices $\{A^{(k)}\}_{k=1}^K$, with $A^{(k)}$ corresponding to latent factor z_k . Note that $A^{(k)}$ has the same dimension as A and Equation 4 presents a trainable weight for each edge, which can be jointly optimized through network training, showcasing an advantage over Equation 3 in this aspect. Therefore, we apply Equation 4 for edge factorization.

Variational Inference: The latent factor variable z determines the quality of node and edge factorization, so we need to approximate its posterior distribution. Denoting $z_u = (z_{u1}, \dots, z_{uK})$, $z_u \in \mathbb{R}_+^K$, which measures how strongly node u is affiliated with all the K latent factors, we adopt a Weibull variational graph encoder [Zhang et al., 2018, He et al., 2022b]:

$$q(z_u | A, X) = \text{Weibull}(k_u, \lambda_u), \quad (k_u, \lambda_u) = \text{GNN}_{\text{EPM}}(A, X), \quad u \in [1, N] \quad (5)$$

where $\text{GNN}_{\text{EPM}}(\cdot)$ stands for graph neural networks, and we select a two-layer Graph Convolution Networks (*i.e.*, GCN [Kipf and Welling, 2016a]) for our models; $k_u, \lambda_u \in \mathbb{R}_+^K$ are the shape and scale parameters of the variational Weibull distribution, respectively. The latent variable z_u can be conveniently reparameterized as:

$$z_u = \lambda_u (-\ln(1 - \varepsilon))^{1/k_u}, \quad \varepsilon \sim \text{Uniform}(0, 1). \quad (6)$$

The optimization objective of latent factor learning phase can be achieved by maximizing the evidence lower bound (ELBO) of the log marginal likelihood of edge $\log p(A)$, which can be computed as:

$$\mathcal{L}_z = \mathbb{E}_{q(Z | A, X)} [\ln p(A | Z)] - \sum_{u=1}^N \mathbb{E}_{q(z_u | A, X)} \left[\ln \frac{q(z_u | A, X)}{p(z_u)} \right] \quad (7)$$

where the first term is the expected log-likelihood or reconstruction error of edge, and the second term is the Kullback–Leibler (KL) divergence that constrains $q(z_u)$ to be close to its prior $p(z_u)$. The analytical expression for the KL divergence and the straightforward reparameterization of the Weibull distribution simplify the gradient estimation of the ELBO concerning the decoder parameters and other parameters in the inference network.

3.3 Disentangled Graph Masked Autoencoder

With the latent factor learning phase discussed in 3.2, the graph can be factorized into a series of factor-specific subgraphs $\{G_1, G_2, \dots, G_K\}$ via the latent factor z . To incorporate the disentangled information encapsulated in z into the graph masked autoencoder, we proposed Disentangled Graph Masked Autoencoder in this section. Specifically, this section will first introduce the latent factor-wise GMAE and the graph-level GMAE.

3.3.1 Latent Factor-wise Graph Masked Autoencoder

To capture disentangled patterns within the latent factor z , for each latent subgraph $\mathcal{G}_k = (V^{(k)}, A^{(k)}, X^{(k)})$, the latent factor-wise GMAE can be described as:

$$H_d^{(k)} = \text{GNN}_{\text{enc}}(A^{(k)}, \bar{X}^{(k)}), \quad \tilde{X}^d = \text{GNN}_{\text{dec}}(A, H_d). \quad (8)$$

where $\bar{X}^{(k)}$ is the masked node feature matrix for the k -th latent factor, and \tilde{X}^d denotes the reconstructed node features. $\text{GNN}_{\text{enc}}(\cdot)$ and $\text{GNN}_{\text{dec}}(\cdot)$ are the graph encoder and decoder, respectively; $H_d^{(k)} \in \mathbb{R}^{N \times D}$ are factor-wise hidden representations, and $H_d = H_d^{(1)} \oplus H_d^{(2)} \dots \oplus H_d^{(K)}$. After the concatenation operation \oplus in feature dimension, the multi factor-wise hidden representation becomes $H_d \in \mathbb{R}^{N \times (K \cdot D)}$, which is used as the input of $\text{GNN}_{\text{dec}}(\cdot)$.

Regarding the mask operation, we uniformly random sample a subset of nodes $\bar{V}^{(k)} \in V^{(k)}$ and mask each of their features with a mask token, such as a learnable vector $X_{[M]} \in \mathbb{R}^d$. Thus, the node feature in the masked feature matrix can be defined as:

$$\bar{X}_i^{(k)} = \begin{cases} X_{[M]}; & v_i \in \bar{V}^{(k)} \\ X_i; & v_i \notin \bar{V}^{(k)}. \end{cases} \quad (9)$$

The objective of latent factor-wise GMAE is to reconstruct the masked features of nodes in $\bar{V}^{(k)}$ given the partially observed node signals $\bar{X}^{(k)}$ and the input adjacency matrix $A^{(k)}$. Another crucial component of the GMAE is the feature reconstruction criterion, often used in language as cross-entropy error [Devlin et al., 2018] and in the image as mean square error [He et al., 2022a]. However, texts and images typically involve tokenized input features, whereas graph autoencoders (GAE) do not have a universal tokenizer. We adopt the scored cosine error of GraphMAE [Hou et al., 2022] as the loss function. Generally, given the original feature $X^{(k)}$ and reconstructed node feature $\tilde{X}^{(k)}$, the defined SCE is:

$$\mathcal{L}_D = \frac{1}{|\bar{V}|} \sum_{i \in \bar{V}} \left(1 - \frac{X_i^T \tilde{X}_i^d}{\|X_i\| \cdot \|\tilde{X}_i^d\|} \right)^\gamma, \quad \gamma \geq 1 \quad (10)$$

where $\bar{V} = \bar{V}^{(1)} \cup \bar{V}^{(2)} \dots \cup \bar{V}^{(K)}$ and Equation 10 are averaged over all masked nodes. The scaling factor γ is a hyper-parameter adjustable over different datasets. This scaling technique could also be viewed as adaptive sample reweighting, and the weight of each sample is adjusted with the reconstruction error. This error is also famous in the field of supervised object detection as the focal loss [Lin et al., 2017].

Graph-level Graph Mask Autoencoder: For the node classification task, we have integrated graph-level GMAE into DiGGR. We provide a detailed experimental analysis and explanation for this difference in Appendix A.1.2. The graph-level masked graph autoencoder is designed with the aim of further capturing the global patterns, which can be designed as:

$$H_g = \text{GNN}_{\text{enc}}(A, \bar{X}), \quad \tilde{X}^g = \text{GNN}_{\text{dec}}(A, H_g). \quad (11)$$

\bar{X} is the masked node feature matrix, whose mask can be generated by uniformly random sampling a subset of nodes $\tilde{V} \in V$, or obtained by concatenating the masks of all factor-specific groups $\tilde{V} = \tilde{V}^{(1)} \cup \tilde{V}^{(2)} \dots \cup \tilde{V}^{(K)}$. The global hidden representation encoded by $\text{GNN}_{\text{enc}}(\cdot)$ is H_g , which is then passed to the decoder. Similar to Equation 10, we can define the graph-level reconstruct loss as:

$$\mathcal{L}_G = \frac{1}{|\tilde{V}|} \sum_{i \in \tilde{V}} \left(1 - \frac{X_i^T \tilde{X}_i^g}{\|X_i\| \cdot \|\tilde{X}_i^g\|} \right)^\gamma, \quad \gamma \geq 1. \quad (12)$$

which is averaged over all masked nodes.

3.4 Joint Training and Inference

Benefiting from the effective variational inference method, the proposed latent factor learning and disentangled graph masked autoencoder can be jointly trained in one framework. We combine the aforementioned losses with three mixing coefficient λ_d , λ_g and λ_z during training, and the loss for joint training can be written as

$$\mathcal{L} = \lambda_d \cdot \mathcal{L}_D + \lambda_g \cdot \mathcal{L}_G + \lambda_z \cdot \mathcal{L}_z. \quad (13)$$

Since Weibull distributions have easy reparameterization functions, these parameters can be jointly trained by stochastic gradient descent with low-variance gradient estimation. We summarize the

training algorithm at Algorithm 1 in Appendix A.4. For downstream applications, the encoder is applied to the input graph without any masking in the inference stage. The generated factor-wise node embeddings H_d and graph-level embeddings H_g can either be concatenated in the feature dimensions or used separately. The resulting final representation H can be employed for various graph learning tasks, such as node classification and graph classification. For graph-level tasks, we use a non-parameterized graph pooling (readout) function, *e.g.*, MaxPooling and MeanPooling to obtain the graph-level representation.

Time and space complexity: Let’s recall that in our context, N , M , and K represent the number of nodes, edges, and latent factors in the graph, respectively. The feature dimension is denoted by F , while L_1 , L_2 , L_3 , and L_4 represent the number of layers in the latent factor learning encoder, the latent factor-wise GMAE’s encoder, the graph-level GMAE’s encoder, and the decoder respectively. In DiGGR, we constrain the hidden dimension size in latent factor-wise GMAE’s encoder to be $1/K$ of the typical baseline dimensions. Consequently, the time complexity for training DiGGR can be expressed as $O((L_1 + L_2 + L_3)MF + (L_1 + L_2/K + L_3)NF^2 + N^2F + L_4NF^2)$, and the space complexity is $O((L_1 + L_2 + L_3 + L_4)NF + KM + (L_1 + L_2/K + L_3 + L_4)F^2)$, with $O((L_1 + L_2/K + L_3 + L_4)F^2)$ attributed to model parameters. We utilize the Bayesian factor model in our approach to reconstruct edges. Its time complexity aligns with that of variational inference in SeeGera Li et al. [2023b], predominantly at $O(N^2F)$; Therefore, the complexity of DiGGR is comparable to previous works.

4 Experiments

We compare the proposed self-supervised framework DiGGR against related baselines on two fundamental tasks: unsupervised representation learning on *node classification* and *graph classification*. We evaluate DiGGR on 11 benchmarks. For node classification, we use 3 citation networks (Cora, Citeseer, Pubmed [Yang et al., 2016]), and protein-protein interaction networks (PPI) [Hamilton et al., 2017]. For graph classification, we use 3 bioinformatics datasets (MUTAG, NCI1, PROTEINS) and 4 social network datasets (IMDB-BINARY, IMDB-MULTI, REDDIT-BINARY and COLLAB). The specific information of the dataset and the hyperparameters used by the network are listed in the Appendix A.2 in table 5 and 6. We also provide the detailed experiment setup in Appendix A.2 for node classification (4.1) and graph classification (4.2)

4.1 Node Classification

The baseline models for node classification can be divided into three categories: *i*) supervised methods, including GCN [Kipf and Welling, 2016a], DisenGCN[Ma et al., 2019], VEPM[He et al., 2022b] and GAT [Velickovic et al., 2017]; *ii*) contrastive learning methods, including MVGRL [Hassani and Khasahmadi, 2020], InfoGCL [Xu et al., 2021], DGI [Veličković et al., 2018], GRACE [Zhu et al., 2020], BGRL [Thakoor et al., 2021] and CCA-SSG [Zhang et al., 2021]; *iii*) generative learning methods, including GraphMAE [Hou et al., 2022], GraphMAE2[Hou et al., 2023], Bandana[Zhao et al., 2024], GiGaMAE[Shi et al., 2023], SeeGera[Li et al., 2023b], GAE and VGAE [Kipf and Welling, 2016b]. The node classification results were listed in Table 1. DiGGR demonstrates competitive results on the provided dataset, achieving results comparable to those of supervised methods.

4.2 Graph Classification

Baseline Models We categorized the baseline models into four groups: *i*) supervised methods, including GIN [Xu et al., 2018], DiffPool[Ying et al., 2018] and VEPM[He et al., 2022b]; *ii*) classical graph kernel methods: Weisfeiler-Lehman sub-tree kernel (WL) [Shervashidze et al., 2011] and deep graph kernel (DGK) [Yanardag and Vishwanathan, 2015]; *iii*) contrastive learning methods, including GCC [Qiu et al., 2020], graph2vec [Narayanan et al., 2017], Infograph [Sun et al., 2019], GraphCL [You et al., 2020], JOAO [You et al., 2021], MVGRL [Hassani and Khasahmadi, 2020], and InfoGCL [Xu et al., 2021]; *iv*) generative learning methods, including graph2vec [Narayanan et al., 2017], sub2vec [Adhikari et al., 2018], node2vec [Grover and Leskovec, 2016], GraphMAE [Hou et al., 2022], GraphMAE2[Hou et al., 2023], GAE and VGAE [Kipf and Welling, 2016b]. Per graph classification research tradition, we report results from previous papers if available.

Table 1: Experiment results for node classification. Micro-F1 score is reported for PPI, and accuracy for other datasets. The best unsupervised method scores in each dataset are highlighted in bold.

Methods	Cora	Citeseer	Pubmed	PPI
GCN [Kipf and Welling, 2016a]	81.50	70.30	79.00	75.70 \pm 0.10
GAT [Veličković et al., 2017]	83.00 \pm 0.70	72.50 \pm 0.70	79.00 \pm 0.30	97.30 \pm 0.20
DisenGCN[Ma et al., 2019]	83.7	73.4	80.5	-
VEPM[He et al., 2022b]	84.3 \pm 0.1	72.5 \pm 0.1	82.4 \pm 0.2	-
MVGRL [Hassani and Khasahmadi, 2020]	83.50 \pm 0.40	73.30 \pm 0.50	80.10 \pm 0.70	-
InfoGCL [Xu et al., 2021]	83.50 \pm 0.30	73.50 \pm 0.40	79.10 \pm 0.20	-
DGI [Veličković et al., 2018]	82.30 \pm 0.60	71.80 \pm 0.70	76.80 \pm 0.60	63.80 \pm 0.20
GRACE [Zhu et al., 2020]	81.90 \pm 0.40	71.20 \pm 0.50	80.60 \pm 0.40	69.71 \pm 0.17
BGRL [Thakoor et al., 2021]	82.70 \pm 0.60	71.10 \pm 0.80	79.60 \pm 0.50	73.63 \pm 0.16
CCA-SSG [Zhang et al., 2021]	84.20 \pm 0.40	73.10 \pm 0.30	81.00 \pm 0.40	73.34 \pm 0.17
GAE [Kipf and Welling, 2016b]	71.50 \pm 0.40	65.80 \pm 0.40	72.10 \pm 0.50	-
VGAE [Kipf and Welling, 2016b]	76.30 \pm 0.20	66.80 \pm 0.20	75.80 \pm 0.40	-
Bandana [Zhao et al., 2024]	84.62 \pm 0.37	73.60 \pm 0.16	83.53 \pm 0.51	-
GiGaMAE[Shi et al., 2023]	84.72 \pm 0.47	72.31 \pm 0.50	-	-
SEGERA [Shi et al., 2023]	84.30 \pm 0.40	73.00 \pm 0.80	80.40 \pm 0.40	-
GraphMAE [Hou et al., 2022]	84.20 \pm 0.40	73.40 \pm 0.40	81.10 \pm 0.40	74.50 \pm 0.29
GraphMAE2[Hou et al., 2023]	84.50 \pm 0.60	73.40 \pm 0.30	81.40 \pm 0.50	-
DiGGR	84.96 \pm 0.32	73.98 \pm 0.27	81.30 \pm 0.26	78.30 \pm 0.71

Table 2: Experiment results in unsupervised representation learning for graph classification. We report accuracy (%) for all datasets. The optimal outcomes for methods, excluding supervised approaches (GIN and DiffPool), on each dataset are emphasized in bold.

Methods	IMDB-B	IMDB-M	MUTAG	NCI1	REDDIT-B	PROTEINS	COLLAB
GIN	75.1 \pm 5.1	52.3 \pm 2.8	89.4 \pm 5.6	82.7 \pm 1.7	92.4 \pm 2.5	76.2 \pm 2.8	80.2 \pm 1.9
DiffPool	72.6 \pm 3.9	-	85.0 \pm 10.3	-	92.1 \pm 2.6	75.1 \pm 3.5	78.9 \pm 2.3
VEPM	76.7 \pm 3.1	54.1 \pm 2.1	93.6 \pm 3.4	83.9 \pm 1.8	90.5 \pm 1.8	80.5 \pm 2.8	-
WL	72.30 \pm 3.44	46.95 \pm 0.46	80.72 \pm 3.00	80.31 \pm 0.46	68.82 \pm 0.41	72.92 \pm 0.56	-
DGK	66.96 \pm 0.56	44.55 \pm 0.52	87.44 \pm 2.72	80.31 \pm 0.46	78.04 \pm 0.39	73.30 \pm 0.82	73.09 \pm 0.25
Infograph	73.03 \pm 0.87	49.69 \pm 0.53	89.01 \pm 1.13	76.20 \pm 1.06	82.50 \pm 1.42	74.44 \pm 0.31	70.65 \pm 1.13
GraphCL	71.14 \pm 0.44	48.58 \pm 0.67	86.80 \pm 1.34	77.87 \pm 0.41	89.53 \pm 0.84	74.39 \pm 0.45	71.36 \pm 1.15
JOAO	70.21 \pm 3.08	49.20 \pm 0.77	87.35 \pm 1.02	78.07 \pm 0.47	85.29 \pm 1.35	74.55 \pm 0.41	69.50 \pm 0.36
GCC	72.0	49.4	-	-	89.9	-	78.9
MVGRL	74.20 \pm 0.70	51.20 \pm 0.50	89.70 \pm 1.10	-	84.50 \pm 0.60	-	-
InfoGCL	75.10 \pm 0.90	51.40 \pm 0.80	91.20 \pm 1.30	80.20 \pm 0.60	-	-	80.00 \pm 1.30
graph2vec	71.10 \pm 0.54	50.44 \pm 0.87	83.15 \pm 9.25	73.22 \pm 1.81	75.78 \pm 1.03	73.30 \pm 2.05	-
sub2vec	55.3 \pm 1.5	36.7 \pm 0.8	61.1 \pm 15.8	52.8 \pm 1.5	71.5 \pm 0.4	53.0 \pm 5.6	-
node2vec	-	-	72.6 \pm 10.2	54.9 \pm 1.6	-	57.5 \pm 3.6	-
GAE	52.1 \pm 0.2	-	84.0 \pm 0.6	73.3 \pm 0.6	74.8 \pm 0.2	74.1 \pm 0.5	-
VGAE	52.1 \pm 0.2	-	84.4 \pm 0.6	73.7 \pm 0.3	74.8 \pm 0.2	74.8 \pm 0.2	-
GraphMAE	75.52 \pm 0.66	51.63 \pm 0.52	88.19 \pm 1.26	80.40 \pm 0.30	88.01 \pm 0.19	75.30 \pm 0.39	80.32 \pm 0.46
GraphMAE2	73.88 \pm 0.53	51.80 \pm 0.60	86.63 \pm 1.33	78.56 \pm 0.26	76.84 \pm 0.21	74.86 \pm 0.34	77.59 \pm 0.22
DiGGR	77.68 \pm 0.48	54.77 \pm 2.63	88.72 \pm 1.03	81.23 \pm 0.40	88.19 \pm 0.28	77.40 \pm 0.05	83.76 \pm 3.70

Performance Comparison The graph classification results are presented in Table 2. In general, we find that DiGGR gained the best performance among other baselines on five out of seven datasets, while achieving competitive results on the other two datasets. The performance of DiGGR is comparable to that of supervised learning methods. For instance, the accuracy on IMDB-B and IMDB-M surpasses that of GIN and DiffPool. Moreover, within the reported datasets, our method demonstrates improved performance compared to random mask methods like GraphMAE, particularly on the IMDB-M, COLLAB, and PROTEINS datasets. This underscores the effectiveness of the proposed method.

Table 3: The NMI between the latent factors extracted by DiGGR and Non-probabilistic factor learning method across various datasets, and its performance improvement compared to GraphMAE, are examined. A lower NMI indicates a more pronounced disentanglement between factor-specific graphs, resulting in a greater performance enhancement.

	Dataset	RDT-B	MUTAG	NCI-1	IMDB-B	PROTEINS	COLLAB	IMDB-M
DiGGR	NMI	0.95	0.90	0.89	0.82	0.76	0.35	0.24
	ACC Gain	+ 0.18%	+ 0.53%	+ 0.83%	+ 2.16%	+ 2.1%	+ 3.44%	+ 3.14%
Non-probabilistic Factor Learning	NMI	1.00	1.00	0.80	1.00	0.60	1.00	0.94
	ACC Gain	-2.23%	-2.02%	-0.45%	-0.80%	-2.15%	-3.00%	-0.11%

4.3 Exploratory Studies

Visualizing latent representations To examine the influence of the learned latent factor on classification results, we visualized the latent disentangled factor z , which reflects the node-factor affiliation, and the hidden representation H used for classification. MUTAG is selected as the representative for classification benchmarks. We encodes the representations into 2-D space via t-SNE [Van der Maaten and Hinton, 2008]. The result is shown in Figure 3(a), where each node is colored according to its node labels. The clusters in Figure 3(a) still exhibit differentiation in the absence of label supervision, suggesting that z obtained through unsupervised learning can enhance node information and offer a guidance for the mask modeling. We then visualize the hidden representation used for classification tasks, and color each node according to the latent factor to which it belongs. The results are depicted in Figure 3(b), showcasing separability among different color clusters. This illustrates the model’s ability to extract information from the latent factor, thereby enhancing the quality of the learned representations.

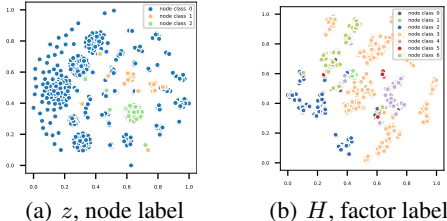


Figure 3: T-SNE visualization of MUTAG dataset, where z is the latent factor, H is the learned node representation used for downstream tasks.

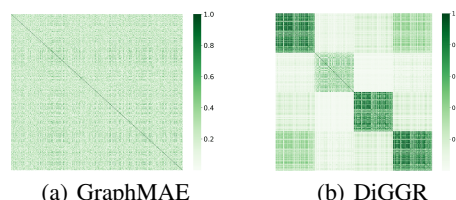


Figure 4: representation correlation matrix on Cora with number of factors $K = 4$. 4(a) depicts the representation of entanglement, while 4(b) illustrates disentanglement.

Task-relevant factors To assess the statistical correlation between the learned latent factor and the task, we follow the approach in [He et al., 2022b] and compute the Normalized Mutual Information (NMI) between the nodes in the factor label and the actual node labels. NMI is a metric that ranges from 0 to 1, where higher values signify more robust statistical dependencies between two random variables. In the experiment, we utilized the MUTAG dataset, comprising 7 distinct node types, and the NMI value we obtained was 0.5458. These results highlight that the latent factors obtained through self-supervised training are meaningful for the task, enhancing the correlation between the inferred latent factors and the task.

Disentangled representations To assess DiGGR’s capability to disentangle the learned representation for downstream task, we provide a qualitative evaluation by plotting the correlation of the node representation in Figure 4. The figure shows the absolute values of the correlation between the elements of 512-dimensional graph representation and representation obtained from GraphMAE and DiGGR, respectively. From the results, we can see that the representation produced by GraphMAE exhibits entanglement, whereas DiGGR’s representation displays a overall block-level pattern, indicating that DiGGR can capture mutually exclusive information in the graph and disentangle the hidden representation to some extent. Results for more datasets can be found in Appendix A.3.

Why DiGGR works better: We provide a **theoretical explanation** for DiGGR’s performance improvement in the Appendix A.5. Additionally, we conduct quantitative experiments here to

demonstrate that disentangled learning can effectively enhance the quality of representations learned by GMAE. The Normalized Mutual Information (NMI) is used to quantify the disentangling degree of different datasets. Generally, the NMI represents the similarity of node sets between different factor-specific graphs, and the *lower NMI suggests a better-disentangled degree* with lower similarity among factor-specific graphs. The NMI between latent factors and the corresponding performance gain (compared to GraphMAE) are shown in the Table.3. As the results show, DiGGR’s performance improvement has a positive correlation with disentangled degree, where the better the disentangled degree, the more significant the performance improvement. For methods relying on Non-probabilistic Factor Learning, the NMI tends to approach 1. This is attributed to the challenges faced by the factor learning module in converging, thereby hindering the learning of distinct latent factors. The presence of confused latent factors offers misleading guidance for representation learning, consequently leading to decreased performance.

5 Conclusions

In this paper, we propose DiGGR (Disentangled Generative Graph Representation Learning), designed to achieve disentangled representations in graph masked autoencoders by leveraging latent disentangled factors. In particular, we achieve this by two steps: 1) We utilize a probabilistic graph generation model to factorize the graph via the learned disentangled latent factor; 2) We develop a Disentangled Graph Masked Autoencoder framework, with the aim of integrating the disentangled information into the representation learning of Graph Masked Autoencoders. Experiments demonstrate that our model can acquire disentangled representations, and achieve favorable results on downstream tasks.

References

Ting Chen, Simon Kornblith, Mohammad Norouzi, and Geoffrey Hinton. A simple framework for contrastive learning of visual representations. In *International conference on machine learning*, pages 1597–1607. PMLR, 2020.

Yuning You, Tianlong Chen, Yongduo Sui, Ting Chen, Zhangyang Wang, and Yang Shen. Graph contrastive learning with augmentations. *Advances in neural information processing systems*, 33: 5812–5823, 2020.

Jacob Devlin, Ming-Wei Chang, Kenton Lee, and Kristina Toutanova. Bert: Pre-training of deep bidirectional transformers for language understanding. *arXiv preprint arXiv:1810.04805*, 2018.

Hangbo Bao, Li Dong, Songhao Piao, and Furu Wei. Beit: Bert pre-training of image transformers. *arXiv preprint arXiv:2106.08254*, 2021.

Kaiming He, Xinlei Chen, Saining Xie, Yanghao Li, Piotr Dollár, and Ross Girshick. Masked autoencoders are scalable vision learners. In *Proceedings of the IEEE/CVF conference on computer vision and pattern recognition*, pages 16000–16009, 2022a.

Qiaoyu Tan, Ninghao Liu, Xiao Huang, Rui Chen, Soo-Hyun Choi, and Xia Hu. Mgae: Masked autoencoders for self-supervised learning on graphs. *arXiv preprint arXiv:2201.02534*, 2022.

Zhenyu Hou, Xiao Liu, Yukuo Cen, Yuxiao Dong, Hongxia Yang, Chunjie Wang, and Jie Tang. GraphMAE: Self-supervised masked graph autoencoders. In *Proceedings of the 28th ACM SIGKDD Conference on Knowledge Discovery and Data Mining*, pages 594–604, 2022.

Wenxuan Tu, Qing Liao, Sihang Zhou, Xin Peng, Chuan Ma, Zhe Liu, Xinwang Liu, and Zhiping Cai. Rare: Robust masked graph autoencoder. *arXiv preprint arXiv:2304.01507*, 2023.

Yijun Tian, Kaiwen Dong, Chunhui Zhang, Chuxu Zhang, and Nitesh V Chawla. Heterogeneous graph masked autoencoders. In *Proceedings of the AAAI Conference on Artificial Intelligence*, volume 37, pages 9997–10005, 2023.

Jianxin Ma, Peng Cui, Kun Kuang, Xin Wang, and Wenwu Zhu. Disentangled graph convolutional networks. In *International conference on machine learning*, pages 4212–4221. PMLR, 2019.

Haoyang Li, Xin Wang, Ziwei Zhang, Zehuan Yuan, Hang Li, and Wenwu Zhu. Disentangled contrastive learning on graphs. *Advances in Neural Information Processing Systems*, 34:21872–21884, 2021.

Yujie Mo, Yajie Lei, Jiale Shen, Xiaoshuang Shi, Heng Tao Shen, and Xiaofeng Zhu. Disentangled multiplex graph representation learning. In *International Conference on Machine Learning*, pages 24983–25005. PMLR, 2023.

Yoshua Bengio, Aaron Courville, and Pascal Vincent. Representation learning: A review and new perspectives. *IEEE transactions on pattern analysis and machine intelligence*, 35(8):1798–1828, 2013.

Teng Xiao, Zhengyu Chen, Zhimeng Guo, Zeyang Zhuang, and Suhang Wang. Decoupled self-supervised learning for graphs. *Advances in Neural Information Processing Systems*, 35:620–634, 2022.

Weihua Hu, Bowen Liu, Joseph Gomes, Marinka Zitnik, Percy Liang, Vijay Pande, and Jure Leskovec. Strategies for pre-training graph neural networks. *arXiv preprint arXiv:1905.12265*, 2019.

Yanqiao Zhu, Yichen Xu, Feng Yu, Qiang Liu, Shu Wu, and Liang Wang. Deep graph contrastive representation learning. *arXiv preprint arXiv:2006.04131*, 2020.

Petar Veličković, William Fedus, William L Hamilton, Pietro Liò, Yoshua Bengio, and R Devon Hjelm. Deep graph infomax. *arXiv preprint arXiv:1809.10341*, 2018.

Kaveh Hassani and Amir Hosein Khasahmadi. Contrastive multi-view representation learning on graphs. In *International conference on machine learning*, pages 4116–4126. PMLR, 2020.

Jiezong Qiu, Qibin Chen, Yuxiao Dong, Jing Zhang, Hongxia Yang, Ming Ding, Kuansan Wang, and Jie Tang. Gcc: Graph contrastive coding for graph neural network pre-training. In *Proceedings of the 26th ACM SIGKDD international conference on knowledge discovery & data mining*, pages 1150–1160, 2020.

Jintang Li, Ruofan Wu, Wangbin Sun, Liang Chen, Sheng Tian, Liang Zhu, Changhua Meng, Zibin Zheng, and Weiqiang Wang. What’s behind the mask: Understanding masked graph modeling for graph autoencoders. In *Proceedings of the 29th ACM SIGKDD Conference on Knowledge Discovery and Data Mining*, pages 1268–1279, 2023a.

Irina Higgins, Loic Matthey, Arka Pal, Christopher P Burgess, Xavier Glorot, Matthew M Botvinick, Shakir Mohamed, and Alexander Lerchner. beta-vae: Learning basic visual concepts with a constrained variational framework. *ICLR (Poster)*, 3, 2017.

Wentao Jiang, Si Liu, Chen Gao, Jie Cao, Ran He, Jiashi Feng, and Shuicheng Yan. Psgan: Pose and expression robust spatial-aware gan for customizable makeup transfer. In *Proceedings of the IEEE/CVF Conference on Computer Vision and Pattern Recognition*, pages 5194–5202, 2020.

Giangiacomo Mercatali, André Freitas, and Vikas Garg. Symmetry-induced disentanglement on graphs. *Advances in neural information processing systems*, 35:31497–31511, 2022.

Mingyuan Zhou. Infinite edge partition models for overlapping community detection and link prediction. In *Artificial intelligence and statistics*, pages 1135–1143. PMLR, 2015.

Zhibin Duan, Dongsheng Wang, Bo Chen, Chaojie Wang, Wenchao Chen, Yewen Li, Jie Ren, and Mingyuan Zhou. Sawtooth factorial topic embeddings guided gamma belief network. In *International Conference on Machine Learning*, pages 2903–2913. PMLR, 2021.

Ioannis Kakogiannou, Spyros Gidaris, Bill Psomas, Yannis Avrithis, Andrei Bursuc, Konstantinos Karantzalos, and Nikos Komodakis. What to hide from your students: Attention-guided masked image modeling. In *European Conference on Computer Vision*, pages 300–318. Springer, 2022.

Yilin He, Chaojie Wang, Hao Zhang, Bo Chen, and Mingyuan Zhou. A variational edge partition model for supervised graph representation learning. *Advances in Neural Information Processing Systems*, 35:12339–12351, 2022b.

Hao Zhang, Bo Chen, Dandan Guo, and Mingyuan Zhou. Whai: Weibull hybrid autoencoding inference for deep topic modeling. *arXiv preprint arXiv:1803.01328*, 2018.

Thomas N Kipf and Max Welling. Semi-supervised classification with graph convolutional networks. *arXiv preprint arXiv:1609.02907*, 2016a.

Tsung-Yi Lin, Priya Goyal, Ross Girshick, Kaiming He, and Piotr Dollár. Focal loss for dense object detection. In *Proceedings of the IEEE international conference on computer vision*, pages 2980–2988, 2017.

Xiang Li, Tiandi Ye, Caihua Shan, Dongsheng Li, and Ming Gao. Seegera: Self-supervised semi-implicit graph variational auto-encoders with masking. In *Proceedings of the ACM web conference 2023*, pages 143–153, 2023b.

Zhilin Yang, William Cohen, and Ruslan Salakhudinov. Revisiting semi-supervised learning with graph embeddings. In *International conference on machine learning*, pages 40–48. PMLR, 2016.

Will Hamilton, Zhitao Ying, and Jure Leskovec. Inductive representation learning on large graphs. *Advances in neural information processing systems*, 30, 2017.

Petar Veličković, Guillem Cucurull, Arantxa Casanova, Adriana Romero, Pietro Lio, Yoshua Bengio, et al. Graph attention networks. *stat*, 1050(20):10–48550, 2017.

Dongkuan Xu, Wei Cheng, Dongsheng Luo, Haifeng Chen, and Xiang Zhang. Infogcl: Information-aware graph contrastive learning. *Advances in Neural Information Processing Systems*, 34: 30414–30425, 2021.

Shantanu Thakoor, Corentin Tallec, Mohammad Gheshlaghi Azar, Mehdi Azabou, Eva L Dyer, Remi Munos, Petar Veličković, and Michal Valko. Large-scale representation learning on graphs via bootstrapping. *arXiv preprint arXiv:2102.06514*, 2021.

Hengrui Zhang, Qitian Wu, Junchi Yan, David Wipf, and Philip S Yu. From canonical correlation analysis to self-supervised graph neural networks. *Advances in Neural Information Processing Systems*, 34:76–89, 2021.

Zhenyu Hou, Yufei He, Yukuo Cen, Xiao Liu, Yuxiao Dong, Evgeny Kharlamov, and Jie Tang. Graphmae2: A decoding-enhanced masked self-supervised graph learner. In *Proceedings of the ACM Web Conference 2023*, pages 737–746, 2023.

Ziwen Zhao, Yuhua Li, Yixiong Zou, Jiliang Tang, and Ruixuan Li. Masked graph autoencoder with non-discrete bandwidths. *arXiv preprint arXiv:2402.03814*, 2024.

Yucheng Shi, Yushun Dong, Qiaoyu Tan, Jundong Li, and Ninghao Liu. Gigamae: Generalizable graph masked autoencoder via collaborative latent space reconstruction. In *Proceedings of the 32nd ACM International Conference on Information and Knowledge Management*, pages 2259–2269, 2023.

Thomas N Kipf and Max Welling. Variational graph auto-encoders. *arXiv preprint arXiv:1611.07308*, 2016b.

Keyulu Xu, Weihua Hu, Jure Leskovec, and Stefanie Jegelka. How powerful are graph neural networks? *arXiv preprint arXiv:1810.00826*, 2018.

Zhitao Ying, Jiaxuan You, Christopher Morris, Xiang Ren, Will Hamilton, and Jure Leskovec. Hierarchical graph representation learning with differentiable pooling. *Advances in neural information processing systems*, 31, 2018.

Nino Shervashidze, Pascal Schweitzer, Erik Jan Van Leeuwen, Kurt Mehlhorn, and Karsten M Borgwardt. Weisfeiler-lehman graph kernels. *Journal of Machine Learning Research*, 12(9), 2011.

Pinar Yanardag and SVN Vishwanathan. Deep graph kernels. In *Proceedings of the 21th ACM SIGKDD international conference on knowledge discovery and data mining*, pages 1365–1374, 2015.

Annamalai Narayanan, Mahinthan Chandramohan, Rajasekar Venkatesan, Lihui Chen, Yang Liu, and Shantanu Jaiswal. graph2vec: Learning distributed representations of graphs. *arXiv preprint arXiv:1707.05005*, 2017.

Fan-Yun Sun, Jordan Hoffmann, Vikas Verma, and Jian Tang. Infograph: Unsupervised and semi-supervised graph-level representation learning via mutual information maximization. *arXiv preprint arXiv:1908.01000*, 2019.

Yuning You, Tianlong Chen, Yang Shen, and Zhangyang Wang. Graph contrastive learning automated. In *International Conference on Machine Learning*, pages 12121–12132. PMLR, 2021.

Bijaya Adhikari, Yao Zhang, Naren Ramakrishnan, and B Aditya Prakash. Sub2vec: Feature learning for subgraphs. In *Advances in Knowledge Discovery and Data Mining: 22nd Pacific-Asia Conference, PAKDD 2018, Melbourne, VIC, Australia, June 3-6, 2018, Proceedings, Part II 22*, pages 170–182. Springer, 2018.

Aditya Grover and Jure Leskovec. node2vec: Scalable feature learning for networks. In *Proceedings of the 22nd ACM SIGKDD international conference on Knowledge discovery and data mining*, pages 855–864, 2016.

Laurens Van der Maaten and Geoffrey Hinton. Visualizing data using t-sne. *Journal of machine learning research*, 9(11), 2008.

Chih-Chung Chang and Chih-Jen Lin. Libsvm: a library for support vector machines. *ACM transactions on intelligent systems and technology (TIST)*, 2(3):1–27, 2011.

Qi Zhang, Yifei Wang, and Yisen Wang. How mask matters: Towards theoretical understandings of masked autoencoders. *Advances in Neural Information Processing Systems*, 35:27127–27139, 2022.

Yao-Hung Hubert Tsai, Yue Wu, Ruslan Salakhutdinov, and Louis-Philippe Morency. Self-supervised learning from a multi-view perspective. *arXiv preprint arXiv:2006.05576*, 2020.

Yonglong Tian, Chen Sun, Ben Poole, Dilip Krishnan, Cordelia Schmid, and Phillip Isola. What makes for good views for contrastive learning? *Advances in neural information processing systems*, 33:6827–6839, 2020.

Reid Andersen, Fan Chung, and Kevin Lang. Local graph partitioning using pagerank vectors. In *2006 47th Annual IEEE Symposium on Foundations of Computer Science (FOCS’06)*, pages 475–486. IEEE, 2006.

A Appendix / supplemental material

Optionally include supplemental material (complete proofs, additional experiments and plots) in appendix. All such materials **SHOULD** be included in the main submission.

A.1 Ablation Study

A.1.1 Number of factors

One of the crucial hyperparameters in DiGGR is the *number of latent factors*, denoted as K . When $K = 1$ DiGGR degenerates into ordinary GMAE, only performing random masking over the entire input graph on the nodes. The influence of tuning K is illustrated in Figure 5. Given the relatively small size of the graphs in the dataset, the number of meaningful latent disentangled factor z is not expected to be very large. The optimal number of z that maximizes performance tends to be concentrated in the range of 2-4.

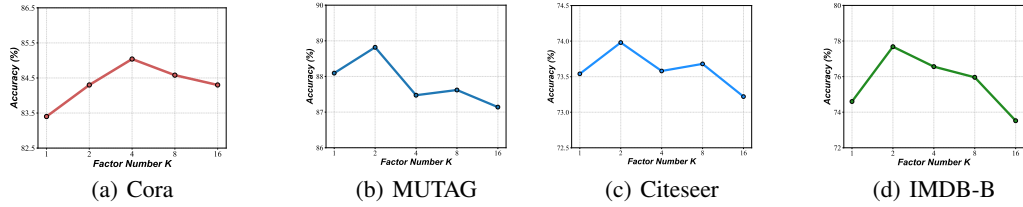


Figure 5: Performance of the task under different choices of latent factor number K , where the horizontal axis represents the change in K and the vertical axis is accuracy.

A.1.2 Representation for downstream tasks

We investigate the impact of various combinations of representation levels on downstream tasks. As illustrated in Table 4, for the node classification task, both H_d and H_g are required, *i.e.*, concatenating them in feature dimension, whereas for the graph classification task, H_d alone is sufficient. This difference may be due to the former not utilizing pooling operations, while the latter does. Specifically, the graph pooling operation aggregates information from all nodes, providing a comprehensive view of the entire graph structure. Thus, in node classification, where the node representation has not undergone pooling, a graph-level representation (H_g) is more critical. In contrast, in graph classification, the node representation undergoes pooling, making disentangled information H_d more effective.

Table 4: Average accuracy of datasets calculated over 5 random initialization tests using different representations.

H_d	H_g	Cora	IMDB-MULTI	Citeseer	PROTEINS
✓		61.10 ± 1.83	54.77 ± 2.63	71.82 ± 0.98	77.76 ± 2.46
	✓	84.22 ± 0.38	51.62 ± 0.61	73.41 ± 0.43	75.52 ± 0.49
✓	✓	84.96 ± 0.32	53.69 ± 2.06	73.98 ± 0.27	77.61 ± 0.97

A.2 Implementation Details

Environment All experiments are conducted on Linux servers equipped with an 12th Gen Intel(R) Core(TM) i7-12700, 256GB RAM and a NVIDIA 3090 GPU. Models of node and graph classification are implemented in PyTorch version 1.12.1, scikit-learn version 1.0.2 and Python 3.7.

Experiment Setup for Node Classification The node classification task involves predicting the unknown node labels in networks. Cora, Citeseer, and Pubmed are employed for transductive learning, whereas PPI follows the inductive setup outlined in GraphSage [Hamilton et al., 2017]. For evaluation,

Table 5: Statistics for node classification datasets.

	Dataset	Cora	Citeseer	Pubmed	PPI
Statistics	# node	2708	3327	19717	56944
	# feature	1433	3703	500	50
	# edges	5429	4732	44338	818736
	# classes	7(s)	6(s)	3(s)	121(m)
Hyper-parameters	Mask Rate	0.5	0.5	0.75	0.5
	Hidden Size	512	512	1024	1024
	Max Epoch	1750	200	1000	1000
	$\lambda_d; \lambda_g; \lambda_z$	1; 1; 1	1; 1; 2	1; 1; 1	1; 1; 1
	Learning Rate	0.001	0.0005	0.001	0.0001
	Factor_Num	4	4	2	2

we use the concatenated representations of H_d and H_g in the feature dimension for the downstream task. We then train a linear classifier and report the mean accuracy on the test nodes through 5 random initializations. The graph encoder $\text{GNN}_{\text{enc}}(\cdot)$ and decoder $\text{GNN}_{\text{dec}}(\cdot)$ are both specified as standard GAT [Velickovic et al., 2017]. We train the model using Adam Optimizer with $\beta_1 = 0.9$, $\beta_2 = 0.999$, $\epsilon = 1 \times 10^{-8}$, and we use the cosine learning rate decay without warmup. We follow the public data splits of Cora, Citeseer, and Pubmed.

Experiment Setup for Graph Classification The graph classification experiment was conducted on 7 benchmarks, in which node labels are used as input features in MUTAG, PROTEINS and NCI1, and node degrees are used in IMDB-BINARY, IMDB-MULTI, REDDIT-BINARY, and COLLAB. The backbone of encoder and decoder is GIN [Xu et al., 2018], which is commonly used in previous graph classification works. The evaluation protocol primarily follows GraphMAE [Hou et al., 2022]. Notice that we only utilize the factor-wise latent representation H_d for the downstream task. Subsequently, we feed it into a downstream LIBSVM [Chang and Lin, 2011] classifier to predict the label and report the mean 10-fold cross-validation accuracy with standard deviation after 5 runs. We set the initial learning rate to 0.0005 with cosine learning rate decay for most cases. For the evaluation, the parameter C of SVM is searched in the set $\{10^{-3}, \dots, 10\}$.

Data Preparation The node features for the citation networks (Cora, Citeseer, Pubmed) are bag-of-words document representations. For the protein-protein interaction networks (PPI), the features of each node are composed of positional gene sets, motif gene sets and immunological signatures (50 in total). For graph classification, the MUTAG, PROTEINS, and NCI1 datasets utilize node labels as node features, represented in the form of one-hot encoding. For IMDB-B, IMDB-M, REDDIT-B, and COLLAB, which lack node features, we utilize the node degree and convert it into a one-hot encoding as a substitute feature. The maximum node degree is set to 400. Nodes with degrees surpassing 400 are uniformly treated as having a degree of 400, following the methodology of GraphMAE[Hou et al., 2022]. Table 5 and Table 6 show the specific statistics of used datasets.

Details for Visualization MUTAG is selected as the representative benchmark for visualization in 4.3. The MUTAG dataset comprises 3,371 nodes with seven node types. The distribution is highly skewed, as 3,333 nodes belong to three types, while the remaining four types collectively represent less than 1.2% of the nodes. For clarity in legend display, we have visualized only the nodes belonging to the first three types.

A.3 Disentangled Representations Visualization

We chose PROTEINS and IMDB-MULTI as representatives of the graph classification dataset, and followed the same methodology as in Section 4.3 to visualize their representation correlation matrices on GraphMAE, and community representation correlation matrices on DiGGR, respectively. The feature dimensions of PROTEINS and IMDB-MULTI are both 512 dimensions, and the number of communities is set to 4.

Table 6: Statistics for graph classification datasets.

	Dataset	IMDB-B	IMDB-M	PROTEINS	COLLAB	MUTAG	REDDIT-B	NCI1
Statistics	Avg. # node	19.8	13.0	39.1	74.5	17.9	429.7	29.8
	# features	136	89	3	401	7	401	37
	# graphs	1000	1500	1113	5000	188	2000	4110
	# classes	2	3	2	3	2	2	2
Hyper-parameters	Mask Rate	0.5	0.5	0.5	0.75	0.75	0.75	0.25
	Hidden Size	512	512	512	256	32	512	1024
	Max Epoch	300	200	50	20	20	200	200
	Learning Rate	0.0001	0.001	0.0005	0.001	0.001	0.0005	0.0005
	$\lambda_d; \lambda_g; \lambda_z$	1; 1; 1	1; 1; 1	1; 1; 1	1; 1; 1	1; 1; 1	1; 1; 1	1; 0.5; 1
	Batch_Size	32	32	32	32	32	16	32
	Pooling_Type	mean	mean	max	max	sum	max	max
	Factor_Num	2	4	4	4	2	2	4

The result is presented in Figure 6. We can see from the results that the graph representations of GraphMAE are entangled. In contrast, the correlation pattern exhibited by DiGGR reveals four distinct diagonal blocks. This suggests that DiGGR is proficient at capturing mutually exclusive information within the latent factor, resulting in disentangled representations.

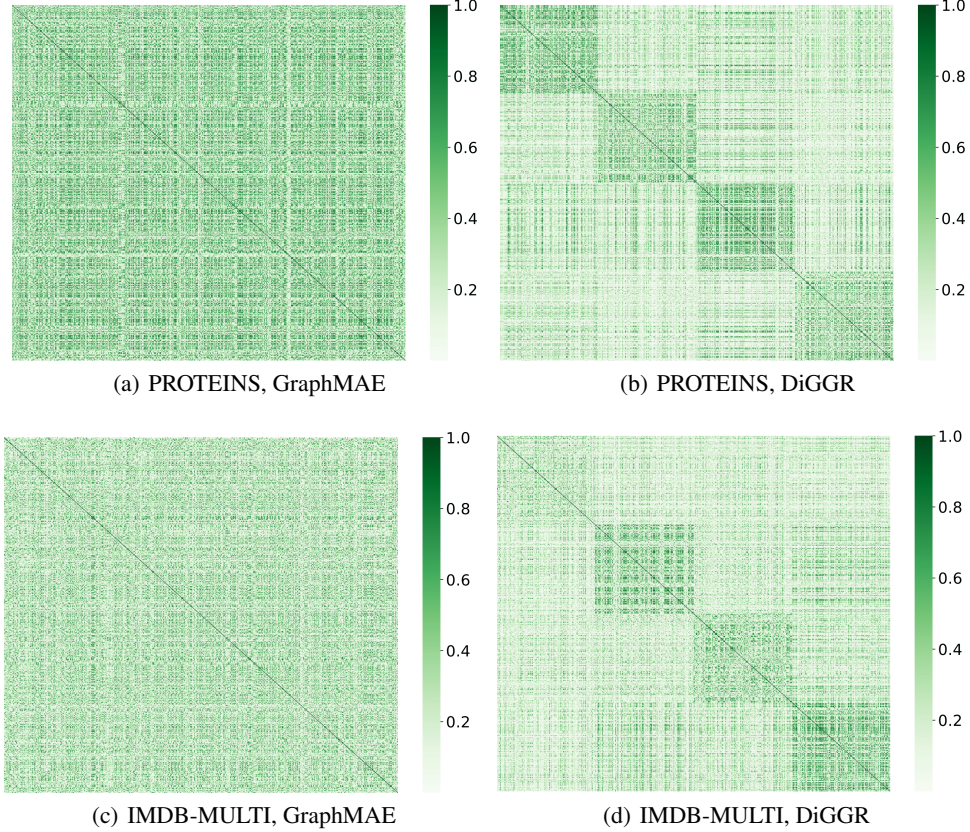


Figure 6: The absolute correlation between the representations learned by GraphMAE and DiGGR is measured on the **PROTEINS** and **IMDB-MULTI** datasets when $K = 4$.

A.4 Training Algorithm

Algorithm 1 The Overall Training Algorithm of DiGGR

- 1: **Input:** Graph $\mathcal{G} = \{V, A, X\}$; latent factor number K .
- 2: **Parameters:** Θ in the inference network of Latent Factor Learning phase, Ω in the encoding network of DiGGR, Ψ in the decoding network of DiGGR.
- 3: Initialize Θ , Ω , and Ψ ;
- 4: **for** iter = 1,2, · · · **do**
- 5: Infer the *variational posterior* of \mathbf{z}_u based on Eq. 5;
- 6: Sample latent factors \mathbf{z}_u from the variational posterior according to Eq. 6;
- 7: Factorize the graph \mathcal{G} into K factor-wise groups $\{\mathcal{G}^{(k)}\}_{k=1}^K$ by node and edge factorization methods;
- 8: Encode $\{\mathcal{G}^{(k)}\}_{k=1}^K$ via latent factor-wise Graph Masked Autoencoder according to Eq. 8;
- 9: Encode \mathcal{G} via graph-level Graph Masked Autoencoder according to Eq. 11;
- 10: Calculate $\nabla_{\Theta, \Omega, \Psi} \mathcal{L}(\Theta, \Omega, \Psi; \mathcal{G})$ according to Eq. 13, and update parameters Θ , Ω , and Ψ jointly.
- 11: **end for**

A.5 Theoretical Approve of Why DiGGR Works

DiGGR is built on an graph autoencoder (GAE)-based framework. Recent studies [Zhang et al., 2022, Li et al., 2023a] have demonstrated a direct connection between GAE and contrastive learning through a specific form of the objective function. The loss function can be rewritten as follows:

$$\begin{aligned} L^+ &= \frac{1}{|\varepsilon^+|} \sum_{(u,v) \in V^+} \log f_{dec}(h_u, h_v) \\ L^- &= \frac{1}{|\varepsilon^-|} \sum_{(u',v') \in V^-} \log(1 - f_{dec}(h_{u'}, h_{v'})) \\ L_{GAE} &= -(L^+ + L^-) \end{aligned}$$

where h_u and h_v are the node representations of node u and node v obtained from an encoder f_{enc} respectively (eg., a GNN); ε^+ is a set of positive edges while ε^- is a set of negative edges sampled from graph, and f_{dec} is a decoder; Typically, $\varepsilon^+ = \varepsilon$.

Building on recent advances in information-theoretic approaches to contrastive learning [Tsai et al., 2020, Tian et al., 2020], a recent study [Li et al., 2023a] suggests that for SSL pretraining to succeed in downstream tasks, task-irrelevant information must be reasonably controlled. Therefore, the following proposition is put forward:

The task irrelevant information $I(U; V|T)$ of GAE can be lower bounded with:

$$I(U; V|T) \geq \frac{(E[N_{uv}^k])^2}{N_k} \cdot \gamma^2$$

minimizing the aforementioned L_{GAE} is in population equivalent to maximizing the mutual information between the k -hop subgraphs of adjacent nodes, and the redundancy of GAE scales almost linearly with the size of overlapping subgraphs.

The above proposition has been proved in detailed in [Li et al., 2023a], where $I(\cdot; \cdot)$ is the mutual information, U and V be random variables of the two contrasting views, and T denote the target of the downstream task. N_{uv}^k is the size of the overlapping subgraph of $G^k(u)$ and $G^k(v)$, and the expectation is taken with respect to the generating distribution of the graph and the randomness in choosing u and v .

According to this lower bound, we need to reduce the task-irrelevant redundancy to design a better graph SSL methods. In DiGGR, we first factorize the input graph based on latent factor learning before feeding it into the masked autoencoder. Take Fig. 7 from the PDF in global rebuttal as an example. Nodes a and b have overlapping 1-hop subgraphs. However, after graph factorization, the

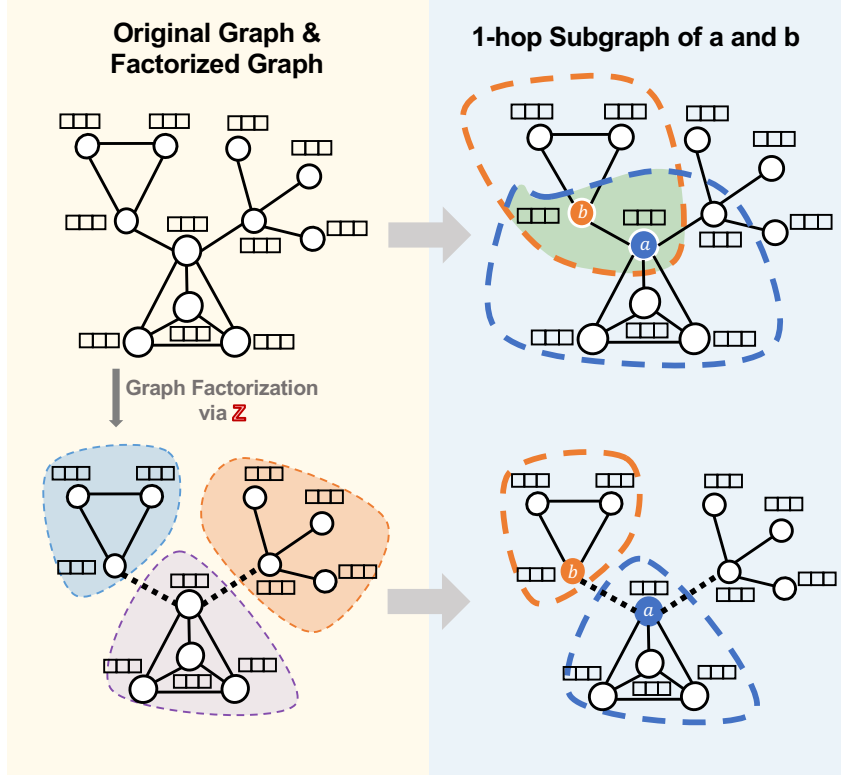


Figure 7: We present examples of 1-hop subgraphs of nodes a and b in both the original and factorized graphs. In the original graph, the 1-hop subgraphs of a and b overlap, as shown by the green area. After applying Graph Factorization, the connection between a and b is cut off, reducing the overlap. This demonstrates that our disentangling method effectively reduces subgraph overlap between nodes, thereby decreasing task-irrelevant information and enhancing the quality of representations obtained through self-supervised learning.

connection between a and b is severed, thereby reducing large-scale subgraph overlap and lowering the lower bound of task-irrelevant information. As shown in Table 3 of the paper, after factorization, the latent factor groups extracted by DiGGR exhibit lower normalized mutual information (NMI), indicating reduced overlap between the latent factor groups. This result aligns with our theoretical analysis and highlights the advantages of our proposed method.

A.6 Broader Impacts

This paper presents work whose goal is to advance the field of Machine Learning. There are many potential societal consequences of our work, none which we feel must be specifically highlighted here.

A.7 Limitations

Despite the promising experimental justifications, our work might potentially suffer from limitation: Although the complexity of the model is discussed in Section 3.4, and it is comparable to previously published work, extending DiGGR to extremely large graph datasets remains challenging at this stage due to the incorporation of an additional probabilistic model into the generative graph framework. One potential solution to this problem could be utilizing PPR-Nibble [Andersen et al., 2006] for efficient implementation, a method that has proven effective in some graph generative models [Hou et al., 2023]. This approach will be pursued in our future work.